Equilibrium Modulus of Model Poly(dimethylsiloxane) Networks

M. Gottlieb,† C. W. Macosko,* and G. S. Benjamin

Department of Chemical Engineering and Materials Science, University of Minnesota, Minneapolis, Minnesota 55455

K. O. Meyers‡ and E. W. Merrill

Department of Chemical Engineering, Massachusetts Institute of Technology, Cambridge, Massachusetts 02139. *Received November 13, 1980*

ABSTRACT: Small-strain, equilibrium modulus data from 12 different studies on poly(dimethylsiloxane) networks are reviewed. For each network enough structural information is available to permit reasonably accurate calculations of the important network parameters: concentration of elastically active strands and junctions and the trapping factor. These are used to compare all the results. The agreement between the various workers is remarkably good. The results support the theoretical concept that topological interactions between PDMS chains contribute directly to the modulus but not greatly to suppression of junction fluctuation.

Recently a number of studies have been done on model rubber networks.[1-19] The goal of these studies has been to test quantitatively the molecular structure basis of the theory of rubber elasticity. In making these networks, each of the investigators endeavored to create a model, covalently linked structure in which the number of strands between junctions and the functionalities of the junctions could be calculated.

One of the major concerns in interpreting results in these studies has been with the influence of topological interactions between chains on mechanical properties of the networks. Several of these studies have been with poly(dimethylsiloxane) (PDMS) networks.[3,5,9-13,15-19] With very similar materials, remarkably different conclusions were reached on the role of chain entanglements. In this paper we review these results and endeavor to reconcile the differences.

We will confine ourselves here only to the small-strain equilibrium modulus, G, of PDMS networks formed and tested in the undiluted state. At small strain the networks should be least disturbed by the measurement. Values for G are available in all the PDMS studies either directly or in terms of constants in the Mooney–Rivlin equation[20,21] used to fit large-strain tensile data. First we review the theoretical relations for G.

Theory for Elastic Modulus

If there are no topological interactions and if the network strands can pass through each other, then the "phantom network" theories of rubber elasticity apply.[22-24] For these theories the shear modulus for networks prepared in bulk becomes

$$G = (\nu - \mu)RT \tag{1}$$

where ν and μ are the concentrations of elastically active strands and junctions. A junction is elastically active if three or more of its arms are independently attached to the network. A strand is elastically active if it is attached at both ends to an active junction.[25] If all strands are attached and there is only one type of junction with functionality f, then

$$\mu = 2\nu/f \tag{2}$$

Thus for a perfect tetrafunctional network eq 1 becomes

$$G = \tfrac{1}{2}\nu RT \tag{3}$$

which is a result that has often been compared to experimental data in the past.[1,21]

In the phantom network, junctions can fluctuate about their mean position due to Brownian motion. This gives rise to the $-\mu$ term in eq 1. The higher the junction functionality, f, the less will be the fluctuations. One manifestation of topological interactions may be to suppress the magnitude of these fluctuations.[26,27] If all junction fluctuation is suppressed, then

$$G = \nu RT \tag{4}$$

which is also the result obtained directly if one assumes that only the network strands give rise to the rubber elasticity force.[28] To allow for intermediate behavior, Dossin and Graessley[8] have used

$$G = (\nu - \mu h)RT \tag{5}$$

where h is an empirical parameter between 0 and 1.

Another approach is to consider that topological interactions can not only suppress junction fluctuation but also raise the free energy of deformation further, as if there were additional cross-links in the network. The idea originates from the observation that linear polymers of high molecular weight behave very much like a cross-linked rubber network over a wide time scale in stress relaxation and other dynamic mechanical tests.[29,30] This is illustrated in Figure 1, which gives dynamic shear modulus vs. small-amplitude oscillation frequency for several high molecular weight PDMS samples[18] and two end-linked PDMS networks.[17] We see that the 10^6 molecular weight linear sample behaves essentially as a cross-linked rubber over a very wide time scale. A small degree of cross-linking, $\nu RT = 1.34 \times 10^5$ Pa, eliminates the long time relaxation but gives a modulus only slightly above the plateau. The plateau modulus, G_N°, of PDMS from these data is 2.4×10^5 Pa, in reasonable agreement with literature values.[31,32]

G_N° appears to be characteristic of the polymer backbone independent of chain length and is taken to be a measure of topological interactions or entanglements between chains. If the chains are cross-linked, it has been proposed that a portion of the interactions which contribute to the plateau modulus will not relax out and this will increase the network modulus. Langley[33] and Graessley and co-workers[8,14] have suggested that these trapped entanglements can be simply added to the small-strain modulus from eq 5

$$G = (\nu - h\mu)RT + G_N^\circ T_e \tag{6}$$

Here T_e is the proportion of the maximum concentration of topological interactions, G_N° which are permanently trapped by the network. Experimentally G_N° depends on

† Present address: Department of Chemical Engineering, Ben-Gurion University, Beer-Sheva, Israel.

‡ Present address: Arco Oil and Gas Co., Dallas, Texas 75221.

0024-9297/81/2214-1039$01.25/0

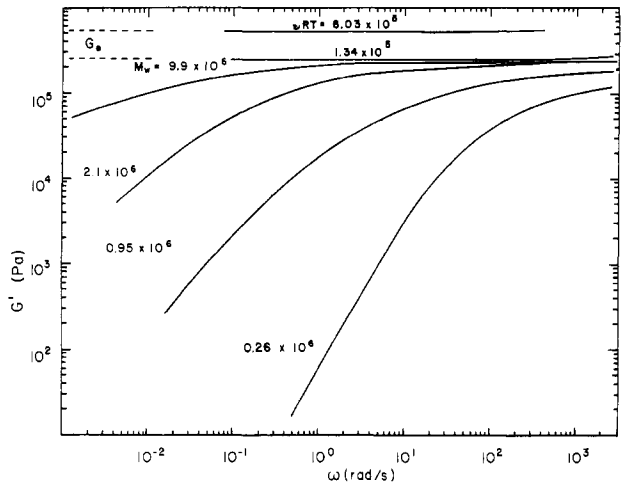

Figure 1. Dynamic shear modulus vs. oscillation frequency for four high molecular weight linear PDMS samples[18] and two tetrafunctionally end-linked networks.[17] The dashed lines indicate the equilibrium modulus of the networks.

the square of polymer concentration, which indicates that it arises from pairwise interactions between chains.[29-31] Thus, T_e can be viewed as the probability that a pairwise interaction is made up of elastically active strands.

Network Parameters

In order to make a careful test of these various relations between network structure and modulus, independent measurements of the network parameters ν, μ, and T_e are required. This has been the major problem in model network studies. If a network is formed in bulk by end-linking and the end-linking reaction is perfect, then ν can be calculated from the average length of the starting chains, M_n, and the bulk density, ρ

$$\nu = \rho/M_n \tag{7}$$

If a purely f-functional end-linking molecule is used, then the junction functionality is just $\mu = 2\nu/f$, eq 2, and since all strands should be linked up, $T_e = 1$.

Most of the previous studies, including some of our own, on model PDMS networks have assumed perfect end-linking and used the above results.[3,4,9-15] This can be dangerous because both ν and T_e are very sensitive to slight incompleteness in the end-linking. This is illustrated in Figure 2 for the formation of a tetrafunctional network. We see that even when end-linking is 90% complete, less than 75% of strands are elastically effective. The trapping factor T_e is even more sensitive to incomplete linking. Clearly, accurate measures of reaction conversion are essential for using model networks to test the molecular aspects of rubber elasticity theory.

Mark and co-workers[5,9] used the reaction of silanol with orthosilicate to end-link PDMS chains. They used Zeisel analysis for the unreacted alkoxy groups but found that this method does not give the accuracy necessary for reliable determination of ν, μ, and T_e. Several studies have used the Pt-catalyzed reaction of SiH with vinyl.[3,10-13,15-19] Valles and Macosko[3,12] attempted to determine the degree of end-linking by monitoring SiH disappearance via infrared spectroscopy. Recently Macosko and Benjamin[18] have shown that SiH can also react slowly with trace amounts of water and thus SiH measurements, particularly for $p_{SiH} > 0.8$, are unreliable. Vinyl groups do not appear to participate in side reactions and can be measured with fair accuracy by iodine chloride or mercuric acetate titration.[34] Recently Llorente and Mark[15] have carried out titration on reacted networks with fair accuracy. Unfortunately, this appears to be the only PDMS network study where conversion was directly measured.

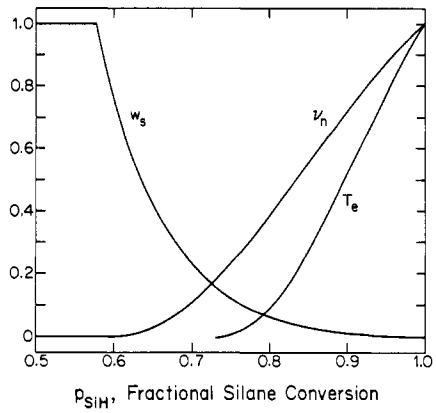

Figure 2. Sol fraction, w_s, concentration of elastically active network chains, ν_n, and trapping factor, T_e, vs. fractional conversion of cross-linker groups for the end-linking of B_2 with A_4 at stoichiometric balance, $r = 1.0$. ν is normalized to ν_n by $\rho RT/M_n$. Plotted from the relations of Miller and Macosko.[12,35,36]

Table I
Comparison of Vinyl Conversion by Sol Fraction and Vinyl Titration[15]

f of network	w_s	$w_s - 0.032$	p_{Vi} calcd	p_{Vi} titration
4	0.035	0.003	0.953	0.952
6[a]	0.035	0.003	0.945	0.851
8[a]	0.035	0.003	0.945	0.944
37[a]	0.061	0.029	0.829	0.775

[a] Mixtures of several functionalities. Equation A-1 was used to calculate p_{Vi} from w_s.

On the other hand, sol fraction data have been reported in nearly all the model network studies. This quantity is directly related to the degree of cross-linking and thus sol data can be used to calculate ν, μ, and T_e. The dependence of w_s on end-linking is illustrated in Figure 2. We note that small changes in w_s reflect large variation in ν. However, with a several-gram network sample and careful methods, it appears possible to determine w_s to ±0.0005.[16,18] The measurements are relatively simple and can be made at any time on the completely formed networks.

A problem with sol fraction measurements has been the presence of nonreactive material in the reactants. The commercially made oligomeric PDMS reactants used in several studies appear to have 2–5% of 300–1500 molecular weight impurities.[12,15-19] Molecular weights less than about 700 can be vacuum stripped.[19] Solvent–nonsolvent fractionation can be used to remove higher molecular weight as was apparently done by Mark and Sullivan.[5,9] Meyers[16] anionically polymerized α,ω-divinyl-PDMS samples which were free of nonreactive species. However, it is not necessary to use these methods to eliminate nonreactive materials. Since the nonreactive species are generally much smaller than the PDMS reactants, GPC can be readily used to determine their concentration in the sol fraction.[16,18] This is shown in Figure 3. We see the nonreactive material as a shoulder in the starting α,ω-divinyl-PDMS, which becomes a separate low molecular weight peak in the sol fraction. By taking chromatogram areas, the nonreactive concentration can be determined and subtracted from the w_s data.

The accuracy of sol fraction measurements for determination of conversion can be tested with the data of Llorente and Mark[15] since they report w_s and independent

Table II
Trifunctional End-Linked PDMS Networks

source	M_n	r	w_{sol}	$10^{-5}G$, Pa	T, K	p_{SiH}	$10^{-5} \times (\nu RT)$, Pa	T_e	$10^{-5} \times (G/T_e)$, Pa	$10^{-5} \times (\nu RT/T_e)$, Pa
Mark, Rahalkar, and Sullivan[9]	32 900	1.00	0.030	0.669	298	0.889	0.286	0.467	1.43	0.62
	25 600		0.029	0.947		0.890	0.377	0.474	2.00	0.80
	18 500		0.030	1.27		0.889	0.508	0.467	2.72	1.09
	9 500		0.011	1.50		0.923	1.41	0.641	2.34	2.20
	4 700		0.030	1.59		0.889	2.00	0.467	3.40	4.28
	4 000		0.021	2.07		0.902	2.66	0.536	3.86	4.96
Valles and Macosko[12]	11 600	0.98		1.92	310	0.93[a]	1.15	0.61	3.2	1.9
		0.997		2.19	300	0.93	1.21	0.67	3.3	1.8
Meyers, Bye, and Merrill[16]	21 600	0.996	0.0180	1.68	298	0.905	0.509	0.535	3.14	0.95
	15 200	1.01	0.0129	2.03		0.915	0.860	0.637	3.19	1.35
	11 100	1.00	0.0281	1.65		0.893	0.882	0.487	3.39	1.81
	8 800	1.00	0.0173	2.10		0.909	1.31	0.570	3.68	2.31
Macosko and Benjamin[18]	39 900	0.99	0.103	0.527	297.0	0.841	0.111	0.214	2.46	0.518
	30 000	1.09	0.0325	1.12	302.0	0.835	0.281	0.451	2.48	0.624
	22 400	0.998	0.073	0.622	285.5	0.853	0.246	0.284	2.19	0.864
	11 400	1.11	0.0073	1.93	298.5	0.861	1.11	0.690	2.80	1.61
		1.21	0.0060	1.92		0.814	1.07	0.731	2.63	1.46
		1.31	0.0040	2.21		0.775	1.05	0.783	2.82	1.34
	5 430	0.986	0.119	0.62	297.5	0.835	0.680	0.182	3.39	3.74
	4 190	1.15	0.0255	1.69	290.5	0.813	1.95	0.502	3.37	3.87
	3 280	1.10	0.0091	2.96	295.0	0.864	3.56	0.672	4.41	5.30

[a] Estimated from w_s data on similar samples.

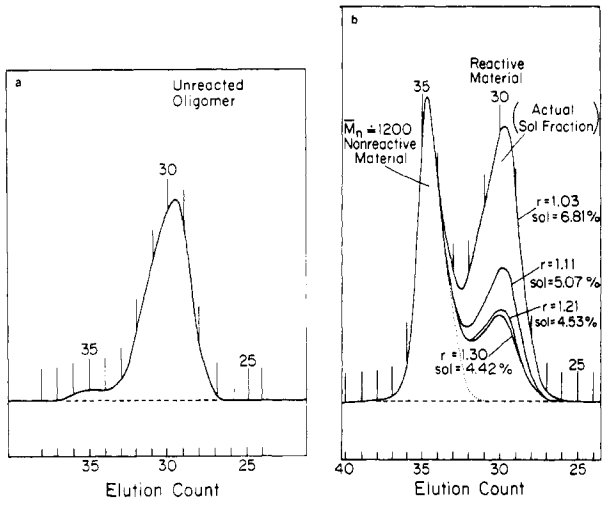

Figure 3. GPC traces of (a) unreacted $B_{2,22}$ and (b) sol fractions of several tetrafunctional networks made with this sample. The shoulder at $M \simeq 1200$ is nonreactive and about 2.8 wt % of the total sample.

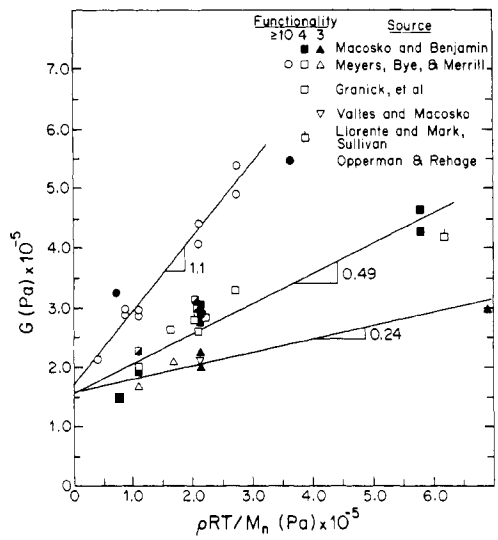

Figure 4. Small-strain modulus vs. reciprocal of oligomer chain length for trifunctional (△), tetrafunctional (□), and high-functionality (○) end-linked networks. Only samples with lowest sol fraction, $w_s < 0.02$, and thus most complete end-linking are included.

measurements of vinyl conversion, p_{Vi}. Table I shows their data. Assuming 3.2% nonreactive species in their α,ω-divinyl-PDMS and subtracting this from the w_s measurements give good agreement with the vinyl titration results. We have found 2.8–3.2% nonreactive material in similar samples from Dow Corning Corp. Vinyl conversion p_{Vi} was calculated from w_s by the relations given in the Appendix.

Comparison of Results

We have collected data from 12 studies on model PDMS networks. These are tabulated in Tables II–V. Small-strain equilibrium modulus data were reported in all studies either directly or as $2C_1 + 2C_2$ from a large-strain, Mooney–Rivlin plot. The later method tends to overestimate G by up to 5%. The network parameters were calculated from the sol fraction data by the relations given in the Appendix. Most of the sol fraction data were corrected for nonreactive material in the original work[12,16-18] or no nonreactive material was believed to be present.[5,9,11,13,16,19] However, as indicated in the tables, some of the w_s values had to be corrected for nonreactive content by using values on similar materials.[15] Some of the w_s data which is not available in the original papers was supplied to us by the authors. One set was estimated from data on other samples in the same paper.[12]

The first comparison of the data is given in Figure 4, showing data for three-, four-, and high-functional end-linked networks. In making this plot, we have used the frequent assumption in these studies: perfect end-linking; thus $\nu = \rho RT/M_n$, eq 7. The points are all for networks with low sol fraction, ≤2%. Although even at this w_s level T_e and ν_n are significantly less than 1.0, especially for the trifunctional networks, we can make two important ob-

Table III
Tetrafunctional End-Linked PDMS Networks

source	M_n	r	w_{sol}	$10^{-5}G$, Pa	T, K	p_{SiH}	$10^{-5} \times (\nu RT)$, Pa	T_e	$10^{-5} \times (G/T_e)$, Pa	$10^{-5} \times (\nu RT/T_e)$, Pa
Mark and Sullivan[5]	45 000	1.00	0.075	0.68	298	0.788	0.185	0.278	2.45	0.65
	32 900		0.046	1.00		0.822	0.335	0.38	2.63	0.88
	25 600		0.017	1.40		0.881	0.618	0.571	2.45	1.08
	18 500		0.06	1.29		0.804	0.517	0.324	3.98	1.60
	9 500		0.03	2.17		0.849	1.38	0.466	4.66	2.97
	4 700		0.034	3.84		0.841	2.63	0.439	8.75	5.98
	4 000		0.012	4.16		0.897	4.185	0.625	6.65	6.70
Llorente and Mark[11]	18 500	1.00	0.075	1.35	298	0.788	0.450	0.278	4.87	1.62
Valles and Macosko[12]	33 400	1.21		1.78	308	0.81[a]	0.62	0.89	2.0	0.70
	11 600	1.00		2.55	313	0.93	1.76	0.74	3.45	2.37
				2.59	300	0.93	1.68	0.74	3.50	2.28
		1.56		1.61	313	0.65	1.42	0.85	1.9	1.7
Llorente and Mark[15]	11 300	1.00	0.005[b]	2.79	298	0.931	1.72	0.744	3.75	2.32
			0.006	2.84		0.925	1.68	0.723	3.98	2.33
			0.004	2.75		0.938	1.77	0.769	3.58	2.30
		1.33[c]	0.003	2.75		0.733	1.50	0.804	3.42	1.86
			0.005	2.76		0.725	1.41	0.752	3.67	1.88
			0.004	2.85		0.728	1.44	0.771	3.70	1.87
Meyers, Bye, and Merrill[16]	21 600	1.12	0.0049	2.40	298	0.845	0.871	0.774	3.10	1.13
	15 200	1.00	0.0081	2.58		0.912	1.19	0.678	3.81	1.76
	11 100	1.10	0.0012	2.94		0.88	1.87	0.866	3.39	2.16
	8 800	1.01	0.0049	3.28		0.933	2.28	0.783	4.19	2.91
Granick et al.[17]	29 200	1.10	0.0288	1.46	293	0.787	0.417	0.473	3.09	0.88
	21 600	0.973	0.0059	2.06	293	0.950	0.888	0.725	2.84	1.23
			0.0048	2.30		0.958	0.913	0.751	3.06	1.21
	21 000	1.10	0.0062	2.25		0.846	0.837	0.718	3.13	1.17
	11 600	1.20	0.0041	3.07		0.794	1.50	0.770	4.00	1.94
			0.0048	2.93		0.790	1.46	0.749	3.91	1.95
			0.0072	2.74		0.781	1.38	0.703	3.90	1.96
	11 400	1.25	0.0077	2.41		0.753	1.34	0.693	3.48	1.94
	3 010	1.20	0.0015	5.00		0.810	6.03	0.855	5.85	7.06
	1 800	1.20	0.0056	8.90	303	0.787		0.734		
Macosko and Benjamin[18]	30 000	1.20	0.0242	1.46	302	0.742	0.416	0.507	2.88	0.819
	22 400	1.11	0.0161	1.76	304	0.807	0.670	0.580	3.03	1.16
	11 400	1.10	0.0025	2.91	299.5	0.868	1.74	0.813	3.58	2.14
		1.18	0.0014	3.03	298.5	0.823	1.73	0.858	3.53	2.01
		1.17	0.0040	2.95	302	0.817	1.65	0.796	3.71	2.07
	4 190	1.20	0.0041	4.61	297	0.793	4.06	0.765	6.03	5.30

[a] Estimated from w_s data on similar samples. [b] 0.030 subtracted from reported w_s data based on content of unreactive materials found in similar samples from Dow Corning Corp. [c] Reported as a trifunctional network.

servations: all the intercepts are positive and the slopes for the tri- and tetrafunctional networks are less than 1. These results suggest that only a model like eq 6 will be able to describe the results. The positive intercept implies a contribution from interchain interactions while the small slopes indicate that junction fluctuation is not completely suppressed in the low-functionality networks.

In Figures 5–7 we plot all of the three-, four-, and high-functional data, now taking into account incomplete end-linking, the last two columns of Tables II–IV. Considering the number of different workers and even chemical systems, the agreement between them is remarkably good. The slopes and intercepts are summarized in Table VI. Note the low standard deviations and the good agreement between the intercepts and G_N° measured independently.

Additional data on randomly cross-linked networks[1,10,19] are shown in Figure 8. Calculation of the network parameters requires different relations, which are also given in the Appendix. We see in the figure that results on networks formed by radiation cross-linking[1] agree well with those prepared by SiH coupling of vinyl groups pendent on the chains.[10,19] Note also the good agreement between the slope and intercept of Figures 8 and 6. This is expected

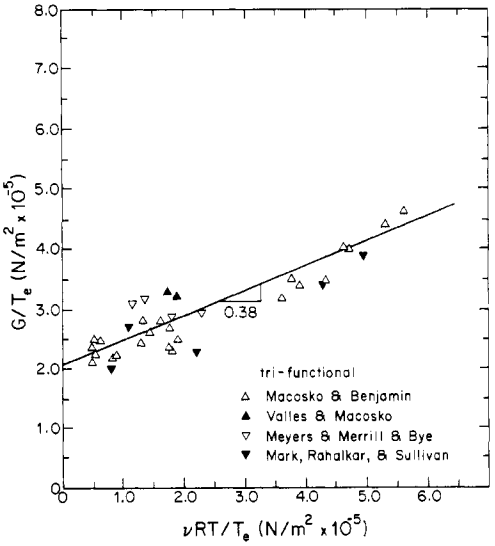

Figure 5. Small-strain modulus vs. concentration of elastically active strands reduced by the factor T_e for all the trifunctional samples, Table II. In calculating ν and T_e, incompleteness of end-linking has been accounted.

Table IV
High-Functionality End-Linked PDMS Networks

source	f	M_n	r	w_{sol}	$10^{-5}G$, Pa	T, K	p_{Vi}	$10^{-5} \times (\nu RT)$, Pa	T_e	$10^{-5} \times (G/T_e)$, Pa	$10^{-5} \times (\nu RT/T_e)$, Pa
Meyers, Bye, and Merrill[16]	24	8 800	1.20	0.0015	5.36	298	0.961	2.48	0.853	6.28	2.91
		9 320	1.21	0.0009	5.33		0.970	2.40	0.884	6.03	2.70
		10 100	1.20	0.0020	4.70		0.955	2.14	0.832	5.65	2.57
		11 100	1.20	0.0015	4.39		0.961	1.98	0.853	5.15	2.32
		12 900	1.20	0.0028	3.85		0.947	1.65	0.803	4.79	2.06
		17 000	1.20	0.0027	3.29		0.948	1.26	0.807	4.08	1.56
		21 600	1.21	0.0022	3.17		0.953	1.01	0.825	3.84	1.22
		28 100	1.16	0.0012	2.98		0.965	0.794	0.868	3.43	0.915
		12 200	1.26	0.0018	4.03		0.957	1.78	0.840	4.80	2.13
		16 300	1.30	0.0103	3.54		0.898	1.18	0.650	5.44	1.81
		20 300	1.65	0.0294	2.27		0.828	0.804	0.469	4.84	1.71
		26 100	1.65	0.0146	1.85		0.879	0.707	0.596	3.10	1.19
		35 400	1.66	0.0148	1.96		0.878	0.521	0.594	3.30	0.877
		51 000	1.42	0.0076	2.11		0.913	0.392	0.694	3.04	0.565
	44	8 800	1.11	0.0017	4.90		0.958	2.47	0.844	5.81	2.93
		10 100	1.27	0.0017	4.51		0.958	2.16	0.844	5.35	2.55
		11 100	1.20	0.0045	3.69		0.932	1.86	0.756	4.88	2.46
		12 900	1.30	0.0021	3.73		0.954	1.68	0.828	4.50	2.03
		17 000	1.31	0.0019	3.29		0.956	1.28	0.836	3.94	1.53
		21 600	1.36	0.0038	2.84		0.938	0.973	0.774	3.67	1.26
		28 100	1.45	0.0033	2.84		0.942	0.756	0.789	3.60	0.96
		12 200	1.30	0.0037	3.99		0.939	1.72	0.777	5.14	2.21
		16 300	1.81	0.0121	3.28		0.889	1.15	0.625	5.25	1.84
		20 300	1.80	0.0228	2.51		0.848	0.844	0.517	4.85	1.63
		26 100	1.80	0.0120	2.29		0.890	0.724	0.627	3.65	1.15
		35 400	1.80	0.0175	2.05		0.867	0.508	0.566	3.62	0.90
		51 000	1.51	0.0105	1.90		0.897	0.379	0.648	2.93	0.58
Llorente and Mark[15]	11	11 300	1.00	0.033	2.98	298	0.885	1.64	0.6	4.86	2.67
				0.033	3.07		0.885	1.64	0.613	5.01	2.67
	37	11 300	1.00	0.061	2.40		0.796	1.34	0.402	6.00	3.32
				0.05	2.71		0.826	1.44	0.465	5.83	3.08
				0.048	2.38		0.832	1.46	0.479	5.00	3.05
Oppermann and Rehage[13]	10	26 000	2.0	<0.003	3.38	298	>0.945	0.821	0.80	4.23	1.03

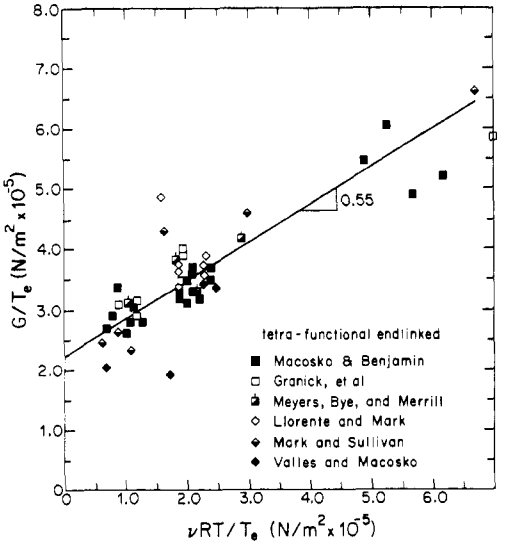

Figure 6. Reduced modulus vs. strand concentration for all the tetrafunctional samples, Table III.

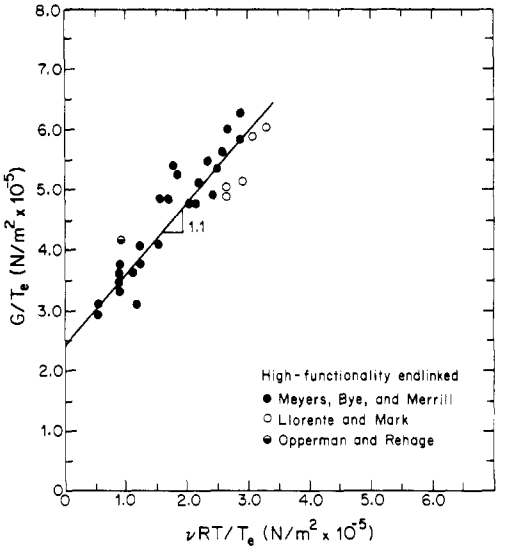

Figure 7. Reduced modulus vs. strand concentration for all the high-functionality samples, Table IV.

from the theory. Structurally, these networks are very similar. Random cross-linking leads to a mixture of three- and four-functional junctions as does incomplete end-linking with a tetrafunctional agent. There have been some arguments against radiation cross-linking because it leads to chain scission and multifunctional junctions.[10] However, it appears that scission can be properly accounted for by using the theoretical relations[37] with sol fraction measurements.

Discussion and Conclusions

We have compared results of 12 different studies from six laboratories on model PDMS networks. The networks were prepared by several chemical reactions and radiation

Table V
Randomly Cross-Linked PDMS Networks

source	r_w	r_w/r_n	w_s	dose, Mrad	$\alpha \times 10^3$	$10^{-5}G$, Pa	$10^{-5} \times (\nu RT)$, Pa	μ/ν	T_e	$10^{-5} \times (G/T_e)$, Pa	$10^{-5} \times (\nu RT/T_e)$, Pa
Langley and Polmanteer[1]	643	1.38	0.225	15.9	4.4[b]	0.34	0.380	0.627	0.063	5.40	6.03
			0.068	31.8	8.8	1.60	1.550	0.599	0.218	7.34	7.11
(M_0 = 74)	1649	1.79	0.082	15.9	4.4	1.13	0.809	0.594	0.244	4.63	3.32
			0.042	31.8	8.8	2.20	2.037	0.574	0.389	5.66	5.24
	4514	2.33	0.050	15.9	4.4	1.70	1.045	0.571	0.415	4.10	2.52
			0.030	31.8	8.8	2.73	2.278	0.560	0.501	5.45	4.55
Falender, Yeh, and Mark[16] (M_0 = 1200)	4883	3.15	*a*		1000[a]	1.78	1.230	0.432	0.850	2.09	1.45
Gottlieb and Macosko[19] (M_0 = 382)	287	3.5	0.204		13.0[c]	0.380	0.278	0.612	0.114	2.26	2.44
			0.169		15.0	0.620	0.384	0.604	0.152	2.99	2.53
			0.108		21.4	1.01	0.734	0.583	0.257	3.93	2.86
			0.066		31.1	1.75	1.319	0.573	0.379	4.62	3.48
			0.048		39.7	2.13	1.826	0.564	0.454	4.69	4.02
			0.040		45.3	2.87	2.166	0.559	0.494	5.81	4.38
			0.025		65.3	4.0	3.402	0.547	0.601	6.67	5.66

[a] Not measured; complete reaction assumed for calculations. [b] Calculated from $\alpha = \alpha_0 D$. [c] Calculated from w_s with eq A-14.

Table VI
Summary of G/T_e vs. $\nu RT/T_e$ Results

type	effective f	$10^{-5} \times$ (intercept),[b] Pa	slope	h
end link	3.0	2.1 ± 0.1	0.38 ± 0.05	0.95[a]
end link	3.6–3.3	2.2	0.55	0.765
random	3.6–3.2	2.5	0.60	0.69
end link	≥10	2.4	1.10	(0)

[a] Using average $\bar{f}$ and $h - (1 - \text{slope})\bar{f}/2$. [b] $G_N^\circ = 2.4 \times 10^5$ Pa.

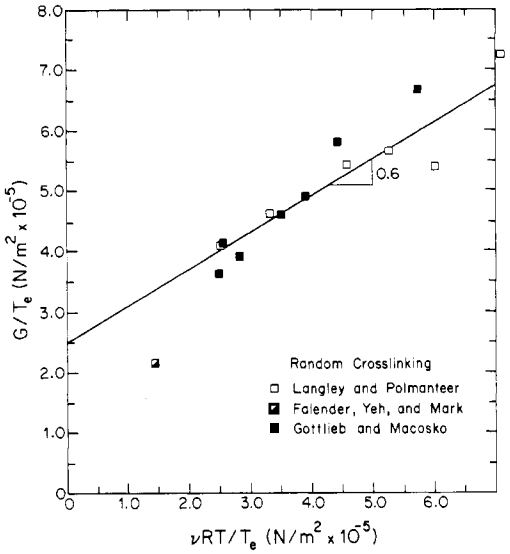

Figure 8. Reduced modulus vs. strand concentration for the randomly cross-linked samples, Table V.

cross-linking. Both random cross-linking and end-linking with a wide range of functionalities and narrow and broad molecular weight distribution precursor chains were used.

All the networks had some degree of incomplete formation. This was accounted for by using branching theory and sol fraction data on each sample. Sol fraction determination of end-group conversion was found to agree with direct titration data when a constant unreactive portion was subtracted from the sol fraction data. With proper accounting of incomplete linking in calculation of the network parameters, we found excellent agreement between small-strain modulus and ν for all the model networks. Of the current rubber elasticity models, eq 6, which includes an additive effect of chain–chain interactions, best describes the results. Suppression of junction fluctuation by chain interactions appears complete for high-functionality networks. For three-functional networks there is very little suppression. Because of incomplete linking the nominally tetrafunctional and randomly cross-linked networks actually have an average functionality of 3.4–3.5. For these networks as indicated by h in Table VI there appears to be some suppression.

Although eq 6 appears to model all PDMS networks, why were different conclusions reached in some of the previous studies? In particular, a number have interpreted their results as showing no influence of chain–chain interactions. Gordon and Roberts[39] based this conclusion on an incomplete set of data from Valles and Macosko.[3] In several studies by Mark and co-workers[5,9–11] fairly incompletely linked networks were interpreted as perfectly end-linked. More recent networks by this group[15] have a much higher degree of end-linking, as can be seen by comparing ref 5 and 11–15 in Table III. However, these data do not cover much range in ν and the comparison to theory emphasized the infinite-strain limit. This limit is not physically attainable and we feel it is only interpretable with respect to a particular theory. It does not have as fundamental a molecular basis as the small-strain limit.

Although the high-functionality networks of Opperman and Rehage[13] agree well with the other studies in Figure 7, they also report data on some nominally tetrafunctional end-linked networks. These had significantly lower modulus than any of the other samples in Table III even when we attempted to account for incomplete linking with w_s data provided by them. These networks were prepared with 25% solvent. This may have reduced chain interaction effects as well as caused errors in subsequent sol fraction measurements.[40]

Equation 6 appears to model the small-strain results on available PDMS model networks quite well and also describes results on several hydrocarbon systems.[8,14] However, a better understanding of the influence of topological interactions is needed. At present the suppression factor h is empirical and the "trapped entanglement" term is more a good correlation between two experiments than a

molecular theory. It is also important to note that eq 6 is only for small strains. A more complete model which includes all stress states such as Flory's[24,27] but which can also describe the small-strain data is needed.

Acknowledgment. This work was supported by a grant from the Army Research Office at the University of Minnesota and the C. P. Dubbs Professorship in Chemical Engineering at the Massachusetts Institute of Technology. Dr. J. R. Fallender and Professors J. D. Ferry, J. E. Mark, and G. Rehage provided data and manuscripts in advance of publication. The comparisons made here would not have been possible without their generous cooperation. We also appreciated helpful discussions with Professor W. W. Graessley and Drs. N. R. Langley and D. S. Pearson.

Appendix. Calculation of ν, μ, and T_e from Sol Fraction Data

Values for ν, μ, and T_e for the end-linked networks given in Tables II and III were calculated from the w_s data by using eq A5–A7 in ref 12. In these equations $[A_f]_0$ is the initial concentration of cross-linking molecules. Since all reactions were done in bulk near room temperature and since the cross-linkers are much smaller than the B_2 oligomers, $[A_f]_0 \simeq r\rho/M_n$, where $\rho = 0.971$ g/cm^3 is the density of PDMS at 25 °C, r is the ratio of the concentration of A to B groups, and M_n is the number-average molecular weight of the B_2 oligomer.

For the high-functionality networks in Table IV we followed the treatment of ref 16, assuming that because of the high functionality the sol fraction consists only of unreacted oligomer. Thus the recursive relations[12,35,36] simplify to

$$w_s = (1 - p_{Vi})^2 w_{B_2} \tag{A-1}$$

where

$$w_{B_2} = M_n/[M_n + (2rM_{A_f})/f]$$

$$\nu = \rho p_{Vi}^2/[M_n + (2rM_{A_f})/f] \tag{A-2}$$

$$T_e = p_{Vi}^4 \tag{A-3}$$

$$\mu = 2\nu/f_e \tag{A-4}$$

where M_{A_f} is the molecular weight of the A_f cross-linker and f_e is its effective functionality

$$f_e = p_{Vi} f/r \tag{A-5}$$

Values of μ, ν, and T_e for the random networks given in Table V were calculated from w_s and radiation dose data, using relations derived by Pearson and Graessley.[8,14,37] For tetrafunctional linkages these relations are

$$\mu = (r\rho/2M_0)(2P_1P_2 + P_2^2) \tag{A-6}$$

$$\nu = (r\rho/2M_0)(3P_1P_2 + 2P_2^2) \tag{A-7}$$

$$T_e = P_2^2 \tag{A-8}$$

$$w_s = 1 - P_1 - P_2 \tag{A-9}$$

where ρ is density, α is the fraction of cross-linkable sites actually linked and M_0 is the molecular weight of the cross-linkable unit on the PDMS chains, and $M_0 = M_n/r_n$. Table V gives the M_0 values. P_1 is the probability that a randomly chosen un-cross-linked unit is connected to the gel by one path and P_2 is the probability that it is connected by two paths:

$$P_1 = [(2 - 2w_s)/\xi](1 - \epsilon) - 2P_2 \tag{A-10}$$

$$P_2 = [(1 - w_s)/\xi]^2[1 - 2\epsilon + (1 + \alpha r_n \xi/b)^{-b-1}] \tag{A-11}$$

Here a Schulz–Zimm form of the molecular weight distribution has been assumed with $b = r_n/(r_w - r_n)$ and r_n is the number average of cross-linkable sites per initial chain. The parameters ϵ and ξ are

$$\epsilon = [1 - (1 + \alpha r_n \xi/b)^{-b}]/\alpha r_n \xi \tag{A-12}$$

and

$$\xi = (1 - w_s) + \beta/\alpha \tag{A-13}$$

where β is the fraction of cross-linkable units which are scissioned during the cross-linking.

For radiation cross-linking α and β can be determined by making a Charlesby–Pinner plot,[38] $w_s + w_s^{1/2}$ vs. $1/Dr_n$. It was assumed that the cross-linking efficiency and scission rate of the radiation were the same for all samples; $\alpha = \alpha_0 D$ and $\beta = \beta_0 D$, with $\alpha_0 = 2.79 \times 10^{-4}$/Mrd and $\beta_0 = 3.4 \times 10^{-5}$/Mrd.

For the random cross-linking of pendent vinyl groups with small SiH molecules, $\beta = 0$. This simplifies the equations, since $\xi = 1 - w_s$, and α can be calculated directly from w_s

$$\alpha = b[w_s^{1/(b+1)} - 1]/r_n(1 - w_s) \tag{A-14}$$

References and Notes

(1) Langley, N. R.; Polmanteer, K. E. *J. Polym. Sci., Polym. Phys. Ed.* **1974**, *12*, 1023.
(2) Morton, M.; Rubio, D. C. Paper No. 43, Rubber Division, American Chemical Society, Cleveland, May 1975. *Rubber Chem. Technol.* **1976**, *49*, 303.
(3) Valles, E. M.; Macosko, C. W. *Rubber Chem. Technol.* **1976**, *49*, 132. *Org. Coat. Plast. Chem.* **1975**, *35* (2), 44. In "Networks: Structure and Properties"; Labana, S. S., Ed.; Academic Press: New York, 1977; p 401.
(4) Allen, G.; Egerton, P. L.; Walsh, D. J. *Polymer* **1976**, *17*, 65.
(5) Mark, J. E.; Sullivan, J. L. *J. Chem. Phys.* **1977**, *66*, 1006.
(6) Herz, J. E.; Rempp, P.; Burchard, W. *Adv. Polym. Sci.* **1978**, *26*, 105 and references therein.
(7) Hinckley, J. A.; Han, C. C.; Mozer, B.; Yu, H. *Macromolecules* **1978**, *11*, 836.
(8) Dossin, L. M.; Graessley, W. W. *Macromolecules* **1979**, *12*, 123.
(9) Mark, J. E.; Rahalkar, R. R.; Sullivan, J. L. *J. Chem. Phys.* **1979**, *70*, 1794.
(10) Falender, J. R.; Yeh, G. S. Y.; Mark, J. E. *J. Chem. Phys.* **1979**, *70*, 5324.
(11) Llorente, M. A.; Mark, J. E. *J. Chem. Phys.* **1979**, *71*, 682.
(12) Valles, E. M.; Macosko, C. W. *Macromolecules* **1979**, *12*, 673.
(13) Oppermann, W.; Rehage, G. Preprints, IUPAC Symposium, Mainz, Sept 1979.
(14) Pearson, D. S.; Graessley, W. W. *Macromolecules* **1980**, *13*, 1001.
(15) Llorente, M. A.; Mark, J. E. *Macromolecules* **1980**, *13*, 681.
(16) Meyers, K. O.; Bye, M. L.; Merrill, E. W. *Macromolecules* **1980**, *13*, 1045. Meyers, K. O. Ph.D. Thesis, Department of Chemical Engineering, MIT, 1980. Bye, M. L. M.S. Thesis, Department of Chemical Engineering, MIT, 1980.
(17) Granick, S.; Pedersen, S.; Nelb, G. W.; Ferry, J. D.; Macosko, C. W. *J. Polym. Sci., Polym. Phys. Ed.*, in press.
(18) Macosko, C. W.; Benjamin, G. S. *Pure Appl. Chem.* **1981**, in press.
(19) Gottlieb, M.; Macosko, C. W.; Lepsch, T. P. *J. Polym. Sci., Polym. Phys. Ed.*, in press.
(20) Mooney, M. *J. Appl. Phys.* **1948**, *19*, 434. Rivlin, R. S. *Philos. Trans. R. Soc. London, Ser. A* **1948**, *241*, 379.
(21) Treloar, L. R. G. "The Physics of Rubber Elasticity", 3rd ed.; Clarendon Press: Oxford, 1975.
(22) Graessley, W. W. *Macromolecules* **1975**, *8*, 186.
(23) Smith, K. J., Jr.; Gaylord, R. J. *J. Polym. Sci., Polym. Phys. Ed.* **1975**, *13*, 2069.
(24) Flory, P. J. *Proc. R. Soc. London, Ser. A* **1976**, *351*, 351.
(25) Scanlan, J. *J. Polym. Sci.* **1960**, *45*, 397.
(26) Ronca, G.; Allegra, G. *J. Chem. Phys.* **1975**, *63*, 4990.
(27) Flory, P. J. *J. Chem. Phys.* **1977**, *66*, 5720.
(28) Flory, P. J. "Principles of Polymer Chemistry"; Cornell University Press: Ithaca, N.Y., 1953.
(29) Ferry, J. D. "Viscoelastic Properties of Polymers", 2nd ed.; Wiley: New York, 1970.
(30) Graessley, W. W. *Adv. Polym. Sci.* **1974**, *16*, 1.
(31) Plazek, D. J.; Dannhuser, W.; Ferry, J. D. *J. Colloid Sci.* **1961**, *16*, 101.
(32) Langley, N. R.; Ferry, J. D. *Macromolecules* **1968**, *1*, 353.
(33) Langley, N. R. *Macromolecules* **1968**, *1*, 348.

(34) Smith, A. L. "Analysis of Silicones"; Wiley: New York, 1974; pp 152, 155.
(35) Miller, D. R.; Macosko, C. W. *Macromolecules* **1976**, *9*, 206.
(36) Miller, D. R.; Valles, E. M.; Macosko, C. W. *Polym. Eng. Sci.* **1979**, *19*, 272.
(37) Pearson, D. S.; Graessley, W. W. *Macromolecules* **1978**, *11*, 528.
(38) Charlesby, A. "Atomic Radiation and Polymers"; Pergamon Press: New York, 1960.
(39) Gordon, M.; Roberts, K. R. *Polymer* **1979**, *20*, 681.
(40) In a paper which appeared after submission of our manuscript, Flory and co-workers (Erman, B.; Wagner, W.; Flory, P. J. *Macromolecules* **1980**, *13*, 1554) used the data of Oppermann and Rehage[13] and Mark and co-workers[10] to argue that the results of Valles and Macosko[12] were in error. Figures 5 and 6 show that when the number of elastically active strands are properly accounted for, the data of Mark's group are in good agreement with those of Valles and Macosko. These studies give significantly higher modulus values than those reported by Oppermann and Rehage for tetrafunctional networks. Experimental errors in making model networks always lead to a lower rather than a higher modulus, if one can exclude the presence of a second phase such as filler particles, precipitate, or stress-induced crystals. It is interesting to note that when the small-strain data of Flory and co-workers on poly(ethyl acrylate) networks are examined (not done in the paper), plots similar to our Figures 4–8 are obtained with a large nonzero intercept.

Radical-Initiated Homo- and Copolymerizations of Chloromethyl Methacrylate

Mitsuru Ueda, Kiyoshi Iri, and Yoshio Imai

Department of Polymer Chemistry, Faculty of Engineering, Yamagata University, Yonezawa, Yamagata 992, Japan

Charles U. Pittman, Jr.*

Department of Chemistry, University of Alabama, University, Alabama 35486.
Received February 17, 1981

ABSTRACT: The kinetics of chloromethyl methacrylate (CMMA) homopolymerization has been investigated in benzene, using azobis(isobutyronitrile) as an initiator. The rate of polymerization (R_p) could be expressed by $R_p = k[\text{AIBN}]^{0.5}[\text{CMMA}]^{1.0}$. The overall activation energy was calculated to be 69.5 kJ/mol. Kinetic constants for CMMA polymerization were obtained as follows: $k_p/k_t^{1/2} = 0.14\ \text{L}^{1/2}\cdot\text{mol}^{-1/2}\cdot\text{s}^{-1/2}$; $2fk_d = 9.4 \times 10^{-6}\ \text{s}^{-1}$. The values of K and a in the Mark–Houwink equation, $[\eta] = KM^a$, were $K = 1.0 \times 10^{-4}$ and $a = 0.725$ when $M = \bar{M}_n$. The relative reactivity ratios of CMMA (M_2) copolymerizations with styrene ($r_1 = 0.21$, $r_2 = 0.31$) and methyl methacrylate ($r_1 = 0.47$, $r_2 = 1.03$) were obtained. Applying the Q–e scheme (in styrene copolymerizations) led to $Q = 1.25$ and $e = 0.85$. This value of e is higher than the value of e for β-chloroethyl methacrylate. Thermogravimetry of poly(CMMA) showed a 10% weight loss at 265 °C in air. The glass transition temperature (T_g) of poly(CMMA) was observed to be 75–80 °C by thermomechanical analysis.

Introduction

Many reports have been published on the correlation between the structure and the reactivity of vinyl monomers in their radical polymerizations and copolymerizations.[1-5] Otsu and co-workers[1] have studied the reactivity of alkyl methacrylates toward the styryl radical and found that their relative reactivities depend on the polar effects of the alkyl groups but not on steric factors. Therefore, the introduction of heteroatoms into the alkyl groups of alkyl methacrylates is expected to increase the polar effects, thereby modifying their reactivities in radical polymerization. However, no detailed study of the radical polymerization of such monomers has been carried out. Thus, we have initiated an investigation of the radical polymerization reactivities of methacrylic esters containing heteroatoms at the α position of alkyl groups. The first such monomer investigated is that containing the chloromethyl group at the α position. The present paper describes kinetic studies of the radical polymerization of CMMA and properties of the resulting polymer. In addition to these results, homo- and copolymers of CMMA are currently being studied for potential lithographic applications.

Experimental Section

Materials. Azobis(isobutyronitrile) (AIBN) was recrystallized from methanol. Benzene was successively washed with concentrated sulfuric acid, dilute sodium hydroxide, and distilled water, dried over calcium chloride, and distilled. The other reagents were used without further purification.

Monomers. Styrene (St) and methyl methacrylate (MMA) were purified by usual methods.

Preparation of Chloromethyl Methacrylate (CMMA). This monomer was prepared according to the procedure of Yakubovich et al.[6] To methacryloyl chloride (40 g, 0.38 mol) and paraformaldehyde (11.5 g, 0.38 mol) was added zinc chloride (1.2 g, 8.8×10^{-3} mol) (ice-bath cooling). After 15 min, the reaction mixture was stirred for 1 h at room temperature and then at 60–65 °C for 1 h. The filtrate was fractionated. After redistillation, 25–33 g (50–65%) of CMMA was obtained: bp 54–55 °C (21 mmHg) [lit.[6] bp 63–65 °C (62 mmHg)]; IR $\nu_{C=O}$ 1740, $\nu_{C=C}$ 1635, ν_{CH_2Cl} 1260 cm^{-1}; NMR (in $CDCl_3$) δ 6.1 (1 H, vinyl protons), 5.6 (1 H, vinyl protons), 5.65 (2 H, methylene protons), 1.95 (3 H, methyl protons); UV (95% ethanol) λ_{max} 208.2 nm (ϵ_{max} 4910).

Homopolymerization of Chloromethyl Methacrylate. Solution Polymerization. CMMA (0.97 g, 7.16 mmol), AIBN (1.8 mg, 1.1×10^{-2} mmol), and 10 mL of dry benzene were charged to a polymerization tube and then degassed (three freeze–thaw–pump cycles). The tube was sealed and heated at 60 °C for 48 h and then opened, and the solution was diluted with benzene. The polymer was precipitated into excess methanol with vigorous stirring. A white fibrous polymer was obtained in >95% yields, exhibiting $[\eta] = 0.57$ dL/g in tetrahydrofuran at 30 °C.

Emulsion Polymerization. Into a 250-mL three-necked flask, fitted with a condenser, a thermometer, a nitrogen inlet, and a magnetic stirrer, were placed 30 mL of distilled degassed water, sodium lauryl sulfate (0.2 g, 6.9×10^{-4} mol), and $K_2S_2O_8$ (0.02 g, 7.4×10^{-5} mol). Nitrogen was passed through the solution for 15 min. Then CMMA (10 g, 0.096 mol) was added and the reaction mixture was heated at 50 °C with vigorous magnetic stirring. After 24 h, the resulting polymer latex was coagulated into 300 mL of methanol. The precipitate was filtered and dried in vacuo overnight at 40 °C to give 8.7 g (87%) of polymer: $[\eta]$

0024-9297/81/2214-1046$01.25/0